

Operation of the Tandem-Mirror Plasma Experiment with Skew Neutral-Beam Injection

T. C. Simonen, S. L. Allen, T. A. Casper, J. F. Clauser, C. A. Clower, F. H. Coensgen, D. L. Correll, W. F. Cummins, C. C. Damm, M. Flammer, J. H. Foote, R. K. Goodman, D. P. Grubb, E. B. Hooper, R. S. Hornady, A. L. Hunt, R. G. Kerr, A. W. Molvik, R. H. Munger, W. E. Nexsen, T. J. Orzechowski, W. L. Pickles, P. Poulsen, M. E. Rensink, B. W. Stallard, and W. C. Turner

Lawrence Livermore National Laboratory, University of California, Livermore, California 94550

and

W. L. Hsu and W. Bauer

Sandia National Laboratory, Livermore, California 94550

and

T. L. Yu and D. Zimmermann

Johns Hopkins University, Baltimore, Maryland 21218

(Received 22 November 1982)

Tandem-mirror plasma with sloshing-ion end plugs has been produced. Ion-velocity distribution functions are peaked at 47° to the magnetic field lines. Low-level ion-cyclotron fluctuations were detected at 1.8 times the plug-midplane frequency and with properties predicted by theory; they did not degrade plasma confinement in the plugs or central cell.

PACS numbers: 52.55.Ke

The tandem mirror employs mirror-confined plasmas at each end of a long central solenoid to generate electrostatic potentials for confining central-cell ions.^{1,2} Tandem-mirror plasmas have been produced by plasma-gun,³ neutral-beam,⁴ and ion-cyclotron-radio-frequency heating.⁵

In our previous tandem-mirror experiment (TMX), the end-plug neutral beams were injected at 90° to the magnetic field lines. In the present experiments (TMX-*U*), we produced a tandem-mirror plasma with sloshing-ion end cells by injecting neutral beams at a skew angle of 47° . For the first time in a beam-driven mirror machine we did not observe fluctuations with the plug-midplane ion-cyclotron frequency. Low-amplitude fluctuations were observed that have the characteristics expected for skew injection. However, we observed no degradation in confinement because of microinstabilities and no heating of escaping central-cell ions by end-plug rf.

When ions are injected at a skew angle θ_0 to the magnetic field lines at the field minimum, they are reflected at a field strength where $B = B_0 / \sin^2 \theta_0$. As they bounce or slosh back and forth, their axial velocity is zero at the point of turnaround, thereby causing the density to peak near the turning points. The lower density near the plug midplane produces an axial potential profile with a dip that electrostatically confines low-

energy ions and aids in stabilizing loss-cone modes.⁶⁻⁹ As with 90° injection, central-cell losses provide additional ions for stability. In the present experiments, this latter unconfined component is an important ingredient in achieving microstability, which will be greatly reduced ultimately in the thermal barrier configuration. A significant feature of the present experiments is that beam injection at an angle also reduces the anisotropy that drives the Alfvén ion-cyclotron mode.¹⁰ Such an angular-velocity distribution function has previously been created in gun-produced plasmas.¹¹⁻¹³

To confine ions injected at 47° in a mirror configuration, the TMX-*U* end plug has a 4:1 mirror ratio^{14,15} [compared to 2:1 in TMX (Ref. 4) and 2XII B (Ref. 16)]. The plug-midplane magnetic field is 0.5 T, and the central-cell field is 0.3 T. The mirror-to-mirror distance of the end plugs is 3 m and of the central cell is 8 m. To maintain minimum-*B* magnetohydrodynamic-stability properties without severe elliptical distortion in the plasma cross section, the magnet generates a radial magnetic well that increases by only 0.5% at the plasma edge, which is shallow compared with 4% in previous experiments.^{4,16} The present experiments show that such shallow wells provide magnetohydrodynamic stability as predicted by theory.¹⁴

Figure 1 shows plug and central-cell plasma

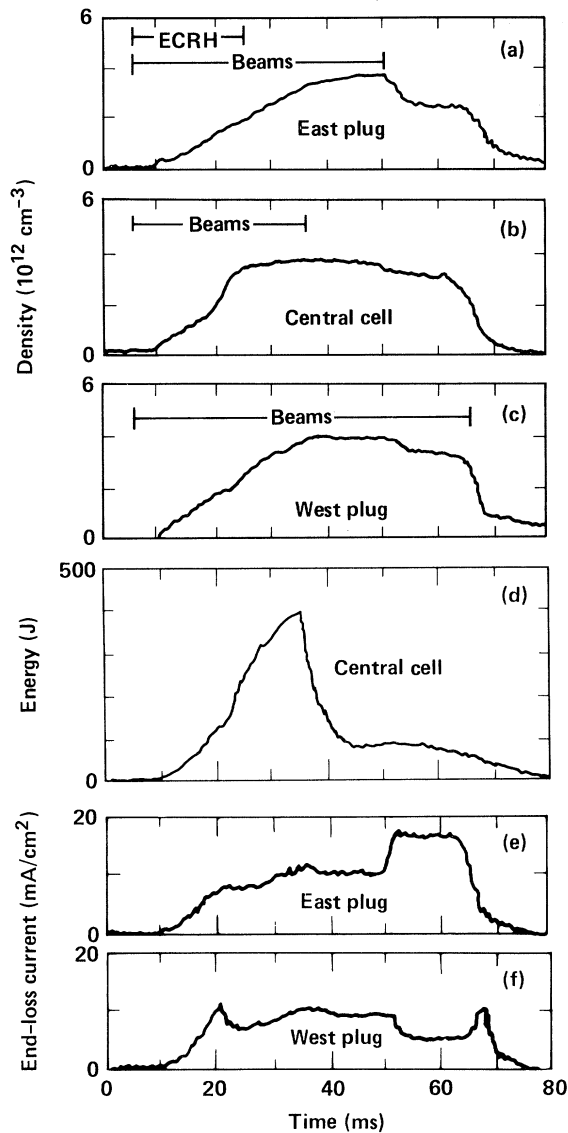


FIG. 1. Diagnostic signals in both east and west-end plugs and in the central cell from TMX-U sloshing-ion experiments: (a) to (c) plasma density; (d) diamagnetic-loop measurement of central-cell energy; and end-loss current density for (e) east and (f) west plugs. Plasma start-up was either by electron-cyclotron-resonant microwave ionization of gas fed into the central cell (ECRH, shown here) or by injection from plasma guns. The plasma density was determined from beam attenuation and microwave interferometer line-density data with use of a 25-cm plug and central-cell diameter.

density, central-cell energy, and end-loss current during the time interval from 0 to 80 ms. The neutral-beam current to each plug and to the central cell was 120 incident atom amperes of deuterons with approximately 11 keV of mean energy. For this shot, neutral beams were turned

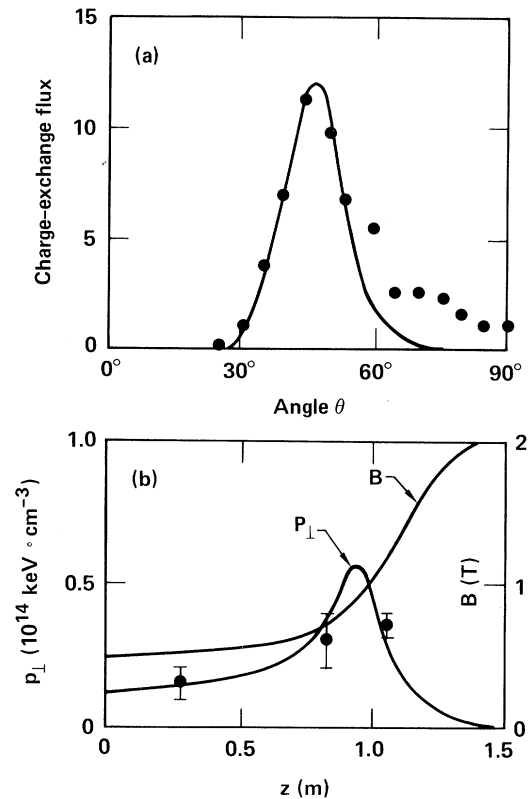


FIG. 2. Measurements from TMX-U of (a) sloshing-ion angular distribution and (b) axial-perpendicular pressure distribution. The bounce-averaged Fokker-Planck-code results shown as solid lines include z -dependent cold-gas charge-exchange losses (0.56 ms at the mirror throat, 5.6 ms at the plug midplane) and a flowing plasma source from the central cell of density $1 \times 10^{12} \text{ cm}^{-3}$ at the plug midplane.

off at different times to diagnose the plasma. When beams are on for their full 75-ms duration, plasma is sustained for the entire beam duration. Densities reach $4 \times 10^{12} \text{ cm}^{-3}$. The mean ion energy of the plugs is 5 keV, composed of 10-keV and 100-eV components with comparable densities. The mean ion energy of the central cell is 2 keV with central-cell neutral-beam injection and ≤ 100 eV without the central-cell beams. The central-cell electron temperature reached 100 eV. Plasma potentials up to 800 V were measured.

When the east-end beams are turned off, the east-end losses increase. The lower west-end-loss current in Fig. 1 indicates electrostatic plugging by the west-end plug. Potential differences between the plug and the central cell can exist at equal densities if the plug electron temperature exceeds that of the central cell. After the east-end beams are turned off, diamagnetic-

loop measurements indicate that the hot ions are lost within 5 ms, as seen in Fig. 1(a). However, the east plug fills up to a density comparable to the central cell.

To establish the existence of sloshing ions we used an angular array of secondary-emission detectors to measure charge-exchange flux. Solid-state and resistance-probe measurements substantiate that the secondary-emission-detector array at 45° measures ≥ 4 -keV ions. In Fig. 2(a) we compare measurements of the angular distribution of sloshing ions with results from a Fokker-Planck code.¹⁷ The distribution remains peaked near 47° , in agreement with the code. The discrepancy near 90° is being investigated.

An axial array of diamagnetic loops also substantiates the presence of sloshing ions. Figure 2(b) shows the axial magnetic field profile for one-half of an end plug. The diamagnetic-loop data show a higher perpendicular pressure near the sloshing-ion turning point than at the mid-plane, in agreement with the code. The skew injection results in a longer hot-ion plasma length of 2 m, compared to 0.4 m in TMX.

To evaluate the microstability of the sloshing-ion distribution for TMX-*U*, we measured ion-cyclotron fluctuations using electrostatic probes¹⁰ in each end plug and in the central cell. The sloshing-ion mode is more microstable than TMX (which operated with 90° beam injection). Even though the level of fluctuations changed by a factor of 3, we observed no change in plasma parameters indicating that the weak fluctuations did not adversely affect the plasma confinement.

With the exception of the sloshing-ion feature, the scale size of TMX-*U* measured in ion gyro-radii (a_i) is actually more vulnerable to micro-instability than TMX. The TMX-*U* has sharper radial density gradients ($r_p/a_i = 4$ rather than 5) and a longer plug length ($L_p/2a_i = 25$ rather than 10). However, TMX-*U* fluctuation amplitudes are smaller (less than 1 V rather than 5) measured at a radius equal to twice the plasma radius. The frequency is that of the ion-cyclotron frequency outside the sloshing-ion density peak where warm ions would not be electrostatically confined. Compared to the Alfvén ion-cyclotron mode, the azimuthal wavelength is smaller and the fluctuations do not propagate to the central cell. All these characteristics are in qualitative agreement with theory for loss-cone-driven modes⁹ and inconsistent with Alfvén ion-cyclotron mode properties, although the roles of electrostatically confined ions and of ions streaming

through the end plugs could not be distinguished.

Further evidence of reduced effects of ion-cyclotron oscillations is seen in the energy spectra¹⁸ of central-cell ions escaping through the end plugs to the end walls as shown in Fig. 3. These data compare TMX and TMX-*U* when both are operating at 0.4-kV plug potential so that loss-cone-microinstability drive is comparable in the absence of warm plasma. In TMX, the central-cell 75-eV escaping ions passing through the plug were heated to 810 eV by the fluctuations.¹⁹ In TMX-*U*, rf heating is hardly measurable.

Diamagnetic measurements in the central cell and end plugs determine the stored plasma energy. From measurements of the plasma radius and assuming a uniform radial temperature profile, we determine on-axis central-cell β 's as high as 10% without observing any limitations or low-frequency activity with increasing central-cell neutral-beam power. Likewise, end-plug β 's up to 4% were measured.

The global energy-confinement time is determined from the ratio of the total stored plasma energy measured by diamagnetic loops to the total beam-power input measured by beam-attenuation diagnostics. With central-cell neutral-beam injection, overall energy-confinement times approaching 5 ms have been observed, which is 3 times longer than in TMX.²⁰ We attribute this im-

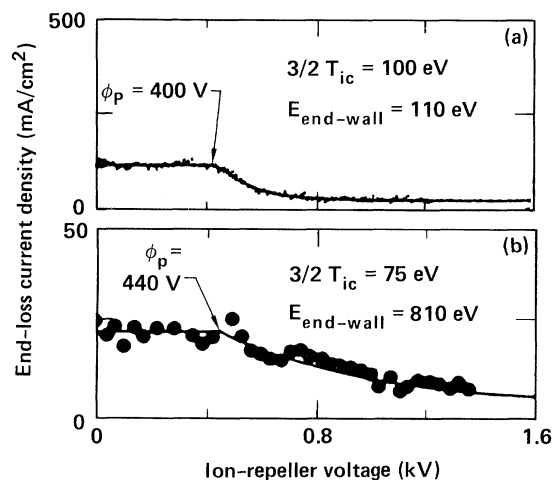


FIG. 3. Energy spectrum of central-cell ions escaping through the end plugs (a) of TMX-*U* and (b) of TMX. The measurements are at comparable central-cell ion temperatures T_{ic} , and plug plasma potentials ϕ_p . The lower energy spread observed at the end wall ($E_{end\ wall}$) in TMX-*U* indicates less rf heating than in TMX. The end-loss current for energies above about 0.8 kV is due to escaping beam-injected sloshing ions.

provement to better vacuum conditions and improved microstability. Our observations are consistent with the dominant energetic particle-loss mechanism being charge exchange on cold gas.

A preliminary assessment of a global power balance without central-cell neutral-beam injection indicates that axial power loss accounts for at least 50% of the trapped beam power. Impurity radiation was small, with impurity concentrations less than 1%, similar to TMX results.

We were able to double central-cell particle confinement with electrostatic plugging. Figure 1 shows that the loss current of the east-end plug increases and that of the west-end plug decreases when the east-end plug is turned off. The maximum ratio that we achieved between the plug and the central-cell density was 2:1, although in Fig. 1 they are about equal. Higher plug densities were limited by the available neutral-beam current. The central-cell density could not be reduced by reducing central-cell fueling without charge-exchange loss of the plug density and subsequent loss of the plasma.

In summary, these experiments point the way to controlling the anisotropy-driven Alfvén ion-cyclotron mode and form a cornerstone for future thermal barrier²¹ experiments. The 2-m-long sloshing-ion plasma is only a factor of 2, both in absolute length and in units of ion gyroradii, smaller than that of fusion-reactor size. The large plasma is sustained at sufficiently low density that microwave heating power can penetrate in future thermal barrier experiments.

This work was performed under the auspices of the U. S. Department of Energy by the Lawrence

Livermore National Laboratory under Contract No. W-7405-ENG-48.

¹T. K. Fowler and B. G. Logan, *Comments Plasma Phys. Controlled Fusion* **2**, 167 (1977).

²G. I. Dimov *et al.*, *Fiz. Plazmy* **2**, 597 (1976) [*Sov. J. Plasma Phys.* **2**, 326 (1976)].

³K. Yatsu *et al.*, *Phys. Rev. Lett.* **43**, 627 (1979).

⁴F. H. Coensgen *et al.*, *Phys. Rev. Lett.* **44**, 1132 (1980).

⁵R. Breun *et al.*, *Phys. Rev. Lett.* **47**, 1833 (1981).

⁶J. Kesner, *J. Plasma Phys.* **15**, 577 (1973).

⁷J. Kesner, *Nucl. Fusion* **20**, 557 (1980).

⁸B. I. Kanaev, *Nucl. Fusion* **19**, 347 (1979).

⁹L. D. Pearlstein, Lawrence Livermore National Laboratory Report No. UCID-19359, 1982 (unpublished).

¹⁰T. A. Casper and G. Smith, *Phys. Rev. Lett.* **48**, 1015 (1982).

¹¹D. Launois, P. Lecoustey, J. Tacher, J. Kesner, and M. Chatelier, *Nucl. Fusion* **12**, 673 (1972).

¹²T. C. Simonen *et al.*, in *Proceedings of the Ninth International Conference on Plasma Physics and Controlled Nuclear Fusion Research*, Baltimore, Maryland, September 1982 (to be published), paper G-1.

¹³M. Inutake *et al.*, in Ref. 12, paper G-3.

¹⁴R. H. Bulmer *et al.*, in Ref. 12, paper G-2.

¹⁵J. H. Foote *et al.*, *J. Fusion Energy* (to be published).

¹⁶W. C. Turner *et al.*, *Nucl. Fusion* **19**, 1011 (1979).

¹⁷T. A. Cutler, L. D. Pearlstein, and M. E. Rensink, Lawrence Livermore National Laboratory Report No. UCRL-52233, 1977 (unpublished).

¹⁸A. W. Molvik, *Rev. Sci. Instrum.* **52**, 704 (1981).

¹⁹R. P. Drake *et al.*, *Nucl. Fusion* **21**, 359 (1981).

²⁰D. P. Grubb *et al.*, to be published.

²¹D. E. Baldwin and B. G. Logan, *Phys. Rev. Lett.* **43**, 1318 (1979).